Supporting Information

Mun et al. 10.1073/pnas.1316001111

SI Materials and Methods

Proteins. F-actin was purified from chicken pectoralis muscle (1). Native thin filaments were purified from porcine cardiac muscle according to Spiess (2), as modified by Matsumoto (3). Bovine cardiac tropomyosin and troponin were produced as described by Tobacman and Adelstein (4). cMyBP-C N-terminal fragments C0C1f (1–269), C0C2 (1–448), and C0C3 (1–539) were bacterially expressed and purified from mouse cardiac cDNA, using the pET expression system (Novagen), as described previously (5).

For the in vitro motility assays, myosin and native thin filaments were freshly isolated from mouse hearts. All protocols complied with the Guide for the Use and Care of Laboratory Animals published by the National Institutes of Health and were approved by the institutional animal care and use committees at University of Vermont Medical School. Wild-type mice of the FVB strain were killed by cervical dislocation. The apex of the heart was removed and was cut into two ∼30-mg pieces. Monomeric myosin was isolated from one piece of the muscle, as previously described (6), and native thin filaments were isolated from the other piece of muscle as follows.

For native mouse cardiac thin filaments, the muscle was immediately placed into a 1.5-mL tube containing 1 mL chilled relaxing solution (50 mM NaCl, 5 mM $MgCl_2$, 2 mM EGTA, 1 mM DTT, 7 mM phosphate buffer at pH 7, 10 mM creatine phosphate, 2.5 mM ATP) and agitated for 1 min by shaking (7). The muscle was transferred with tweezers (Dumont #5, Biologie Tips) to a dissecting chamber containing 1 mL chilled relaxing solution with 0.5% Triton-X 100 and then teased into 3–5-mm strips, using the tweezers. The muscle strips were transferred with the tweezers into a 0.2-mL glass tissue homogenizer (Kontes, Fisher Scientific) containing 150 μL homogenization buffer (100 mM KCl, 5 mM $MgCl_2$, 1 mM EGTA, 25 mM imidazole at pH 6.45, 10 mM DTT, 5 mM ATP, and 0.1% Triton X-100) and homogenized on ice for 15 min. The homogenate was centrifuged in a TLA-100 rotor (Beckman, Coulter) (20 min, 40,000 × *g*). The supernatant was transferred into a new centrifuge tube and recentrifuged (45 min, 200,000 × *g*). The supernatant was discarded; the pellet was resuspended in 75 μL of 100 mM KCl, 5 mM $MgCl_2$, 1 mM EGTA, 25 mM imidazole (pH 7.9), 10 mM DTT, and 5 mM ATP; and the suspension was centrifuged (5 min, 40,000 × *g*). The supernatant was transferred to a new centrifuge tube and recentrifuged (45 min, 200,000 × *g*). The pellet, which contained the native thin filaments, was softened overnight with 10 μL homogenization buffer without ATP or Triton X-100. The following morning, the total protein concentration was determined using a Bradford assay (Bio-Rad), and the actin concentration was estimated from the total protein content, assuming the presence of 7 actin monomers per troponin and tropomyosin complex. The native thin filaments were fluorescently labeled by mixing 10 μM actin with 10 μM tetramethyl-rhodamine-phalloidin in homogenization buffer without ATP or Triton X-100 (ice, 1 h). The labeled native thin filaments were diluted to 5 nM in actin buffer (AB) [25 mM KCl, 1 mM EGTA, 10 mM DTT, 25 mM imidazole, 4 mM $MgCl_2$, adjusted to pH 7.4; containing an oxygen scavenging system (0.1 μg/mL glucose oxidase, 0.018 μg/mL catalase, 2.3 μg/mL glucose)] before use.

Electron Microscopy. Two micromolar native thin filaments, or 2 μM F-actin preincubated with tropomyosin and troponin (7:2:2 = F-actin:Tm:Tn) (8) were mixed with 0.3–12 μM C0C2 (1:6, 1:3, 1:1, or 7:1 ratio = actin subunits: C0C2) under three different buffer conditions, each of which has been used in previous thin filament studies. The major difference between them was the KAc/NaCl concentration, and hence the ionic strength (1). One hundred millimolar KAcetate, 2 mM $MgCl_2$, 0.2 mM EGTA, 1 mM DTT, 10 mM Mops at pH 7.0 (9); (2) 100 mM NaCl, 3 mM $MgCl_2$, 0.2 mM EGTA, 1 mM NaN_3, 5 mM sodium phosphate, 5 mM Pipes at pH 7.1 (5, 8); (3) 180 mM KAcetate, 2 mM $MgCl_2$, 0.2 mM EGTA, 1 mM DTT, 10 mM Mops at pH 7.0 (10). After mixing, solutions were incubated at room temperature for 30 min. For high Ca^{2+} conditions, 0.33 mM $CaCl_2$ was added to the appropriate buffer. Five-microliter aliquots were then applied to EM grids coated with thin carbon supported by a holey carbon film and negatively stained with 1% (wt/vol) uranyl acetate (11). Dried grids were observed in a Philips CM120 electron microscope (FEI) at 80 KV under low-dose conditions. Images of filaments were acquired at a pixel size of 0.35 nm, using a 2K × 2K CCD camera (F224HD, TVIPS GmbH).

3D Reconstruction. Long, relatively straight thin filaments were chosen for 3D reconstruction and unbent using ImageJ. Selected filament regions were converted to SPIDER format (EM2EM; Image Science and Imperial College, London, United Kingdom), and cut into segments in SPIDER (v11.2; Wadsworth Center). Iterative helical real-space reconstruction was carried out using SPIDER (12, 13). An F-actin model (no tropomyosin) was used as an initial reference model for the first round of iterative helical real-space reconstruction so that the model would not bias the position of Tm in the reconstruction (similar results were obtained using a uniform cylinder as the reference). Filament segments were fitted to different rotational views of the reference represented by 90 2D projections of the model turned 360° in 4° intervals. Cross-correlation and alignment were performed between the filament segments and the projections, using the AP NQ routine in SPIDER. Segments aligning with incorrect polarity or with in-plane rotations greater than ± 4° from their preset vertical orientation were discarded, and the remaining segments were back-projected using the SPIDER BP 3F routine. A search for helical symmetry was performed, and the symmetrized reconstruction was used as a reference model for the next round of alignment and image reconstruction (13). The process was iterated for 20 rounds, with convergence (no changes from one round to the next) generally occurring within 10 rounds. The resulting reconstructions had resolutions between 1.6 and 3.2 nm, according to the Fourier shell correlation 0.5 criterion, with the higher resolutions being obtained for the undecorated filaments. UCSF Chimera (14) was used for visualization, analysis, and atomic fitting of 3D volumes.

Comparison and Atomic Fitting of Reconstructions. Accurate matching of reconstructions to each other was essential to determine whether cMyBP-C N-terminal fragments caused tropomyosin movement. Matching was carried out using an F-actin reconstruction as a reference to which all other reconstructions were fitted. This matching was done using the highest-density region of actin in both the experimental and reference F-actin structures (the SD1 region in all cases) as the guide to the superposition. After adjusting the two reconstructions to a high-contour cutoff, an approximate fit was carried out manually; this was then optimized using the "fit in map" tool of Chimera, which shifts and rotates the reconstruction relative to the F-actin reference to maximize their correlation. Using this approach, only the densities greater than or equal to the high-contour cutoff selected are used for matching; the

lower-density tropomyosin and C0C2 contributions are ignored and do not influence the fitting. After fitting, the contour cutoff was lowered so that tropomyosin and the outer surface of F-actin in the experimental reconstruction became visible. Comparison of different experimental reconstructions, all fitted to the same reference F-actin model, revealed any changes in tropomyosin position. The same fitting was obtained using a variety of different high-contour cutoffs, showing that the exact choice of cutoff was not critical. Comparison of control low and high Ca^{2+} filaments shows that this approach works by demonstrating the known shift of tropomyosin in response to Ca^{2+} (Fig. 3).

The reconstructions were fitted with atomic models of F-actin and/or F-actin-tropomyosin determined by X-ray diffraction and cryo-EM (15, 16). First, the reconstruction of F-actin alone was fitted to the F-actin atomic model, using the Chimera "fit in map" tool, as described earlier. A surface contour of the reconstruction was then chosen that enclosed the atomic model with minimal projection of actin density outside of the envelope. To compare the positions of the tropomyosin strands in the experimental reconstructions with the known high and low Ca^{2+} positions of tropomyosin in the atomic model, the experimental reconstruction was made translucent and the atomic model (fitted to F-actin as above) was made visible within it, revealing the position of tropomyosin in the atomic model (e.g., Figs. 3 *A* and *B* and 4 *A*–*C*). Because all reconstructions were fitted to the same reference F-actin model, the atomic fitting was standardized across all reconstructions.

In Vitro Motility. In vitro motility assays were performed on the surface of a nitrocellulose-coated flow cell, and the motion of actin filaments was observed by epifluorescence microscopy, similar to that previously described (17). In short, 100 μg/mL mouse cardiac myosin was incubated in the flow cell (2 min), and then the surface of the flow cell was blocked by the addition of two aliquots of BSA (1 mg/mL in AB). Next, two aliquots of 1 μM unlabeled native thin filaments in AB were added to the flow cell (1 min). The flow cell was rinsed two times with 1 mM ATP in AB to eliminate myosin that irreversibly binds actin in an ATP-insensitive manner (17), and then two more times with AB. Two aliquots of tetramethyl-rhodamine-phalloidin-labeled native thin filaments were added to the flow cell (1 min), and then the flow cell was rinsed three times with AB. Motility buffer [AB containing 100 μM ATP, 0.5% methyl cellulose, calcium chloride ranging from negative log of calcium concentration (pCa) 4–9, and 1 μM of either C0C1f or C0C3 (where applicable)] was added to the flow cell, and actin filament motion was observed by epifluorescence microscopy at 22 °C after 3 min incubation. Calcium levels were determined using MaxChelator software (18) to account for the 1 mM EGTA present in the motility buffer.

A Lumen 200W metal arc lamp (Prior Scientific) was used for fluorescent excitation, a Nikon Eclipse Ti-U microscope equipped with a PlanApo objective lens (100×, 1.35 n.a.) and an intensified high-resolution Mega Z 10-bit digital camera (Stanford Photonics), using Piper software, were used to acquire the images at 10 frames/s without pixel binning (95 nm/pixel). The image stacks were down-sampled to 2 frames/s, using Image J 1.43u (National Institutes of Health), and DiaTrack 3.03 software for Windows (Semasopht) was used for data analysis. The velocity of each moving actin filament and percentage of motile filaments were determined in each movie. The mean velocity and fraction moving were determined from four movies for each experimental condition, and the product was determined. The mean velocity × fraction of moving filaments ± SEM from three independent experiments were determined. Velocity × fraction of moving filaments were plotted with respect to pCa, fitted with a sigmoidal dose–response curve, and the pCa_{50} used to determine changes in calcium sensitivity.

1. Pardee JD, Spudich JA (1982) Purification of muscle actin. *Methods Enzymol* 85(Pt B): 164–181.
2. Spiess M, et al. (1999) Isolation, electron microscopic imaging, and 3-D visualization of native cardiac thin myofilaments. *J Struct Biol* 126(2):98–104.
3. Matsumoto F, et al. (2004) Conformational changes of troponin C within the thin filaments detected by neutron scattering. *J Mol Biol* 342(4):1209–1221.
4. Tobacman LS, Adelstein RS (1986) Mechanism of regulation of cardiac actin-myosin subfragment 1 by troponin-tropomyosin. *Biochemistry* 25(4):798–802.
5. Mun JY, et al. (2011) Electron microscopy and 3D reconstruction of F-actin decorated with cardiac myosin-binding protein C (cMyBP-C). *J Mol Biol* 410(2): 214–225.
6. Debold EP, et al. (2007) Hypertrophic and dilated cardiomyopathy mutations differentially affect the molecular force generation of mouse alpha-cardiac myosin in the laser trap assay. *Am J Physiol Heart Circ Physiol* 293(1):H284–H291.
7. Lehman W, Vibert P, Uman P, Craig R (1995) Steric-blocking by tropomyosin visualized in relaxed vertebrate muscle thin filaments. *J Mol Biol* 251(2):191–196.
8. Pirani A, et al. (2005) Single particle analysis of relaxed and activated muscle thin filaments. *J Mol Biol* 346(3):761–772.
9. White HD, Belknap B, Harris SP (2013) Activation and inhibition of F-actin and cardiac thin filaments by the N-terminal domains of cardiac myosin binding protein C. *Biophys J* 104(2):158a–159a.
10. White HD, Harris S (2012) Activation of cardiac thin filaments by N-terminal domains of cardiac myosin binding protein C. *Biophys J* 102(3):435a.
11. Craig R, Lehman W (2001) Crossbridge and tropomyosin positions observed in native, interacting thick and thin filaments. *J Mol Biol* 311(5):1027–1036.
12. Frank J, et al. (1996) SPIDER and WEB: Processing and visualization of images in 3D electron microscopy and related fields. *J Struct Biol* 116(1):190–199.
13. Egelman EH (2000) A robust algorithm for the reconstruction of helical filaments using single-particle methods. *Ultramicroscopy* 85(4):225–234.
14. Pettersen EF, et al. (2004) UCSF Chimera—a visualization system for exploratory research and analysis. *J Comput Chem* 25(13):1605–1612.
15. Holmes KC, Angert I, Kull FJ, Jahn W, Schröder RR (2003) Electron cryo-microscopy shows how strong binding of myosin to actin releases nucleotide. *Nature* 425(6956): 423–427.
16. Poole KJ, et al. (2006) A comparison of muscle thin filament models obtained from electron microscopy reconstructions and low-angle X-ray fibre diagrams from non-overlap muscle. *J Struct Biol* 155(2):273–284.
17. Palmiter KA, et al. (2000) R403Q and L908V mutant beta-cardiac myosin from patients with familial hypertrophic cardiomyopathy exhibit enhanced mechanical performance at the single molecule level. *J Muscle Res Cell Motil* 21(7):609–620.
18. Patton C, Thompson S, Epel D (2004) Some precautions in using chelators to buffer metals in biological solutions. *Cell Calcium* 35(5):427–431.

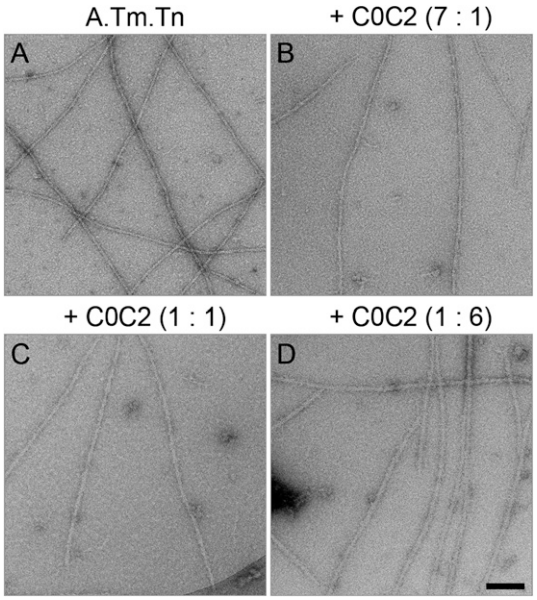

Fig. S1. Comparison of reconstituted thin filaments decorated with different ratios of C0C2 in low Ca^{2+} conditions. (*A*) Thin filament control. (*B–D*) Filaments decorated with C0C2 at the A:C0C2 molar ratios indicated. (Scale bar = 100 nm.)

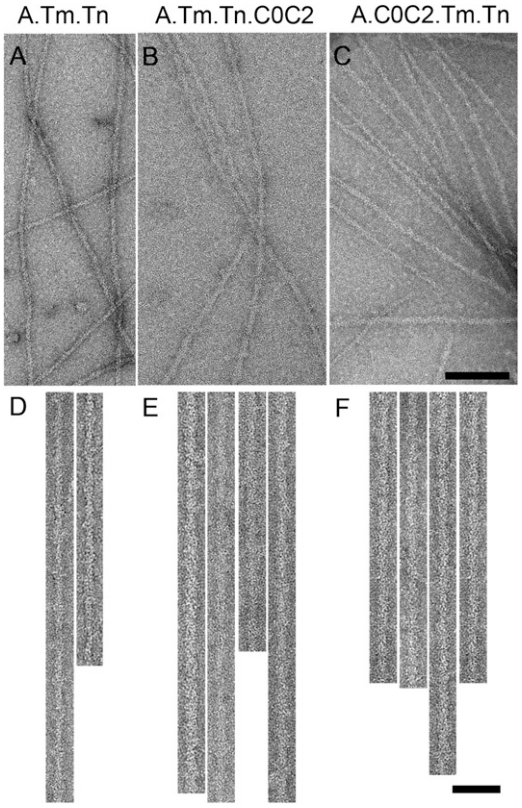

Fig. S2. Decoration of low Ca^{2+} reconstituted thin filaments using different mixing orders. (*A*, *D*) Reconstituted thin filament control. (*B*, *C*, *E*, *F*) Filaments decorated with C0C2, added after (*B*, *E*) or before (*C*, *F*) Tm.Tn. Filaments in *D–F* have been computationally straightened. [Scale bar (*A–C*) = 100 nm; (*D–F*) = 50 nm.]

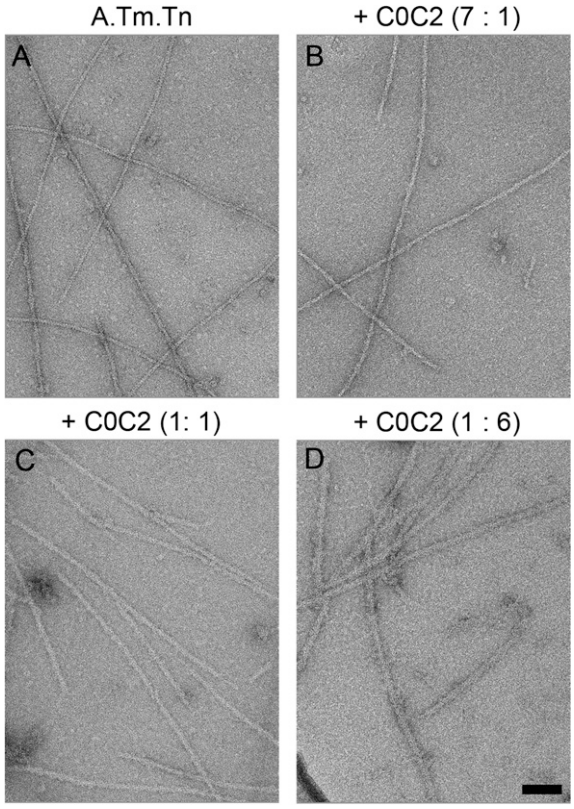

Fig. S3. Comparison of C0C2-decorated thin filaments under high Ca^{2+} conditions at different A:C0C2 ratios. (*A*) Thin filament control; (*B–D*) Filaments decorated with C0C2 at the ratios indicated. (Scale bar = 50 nm.)

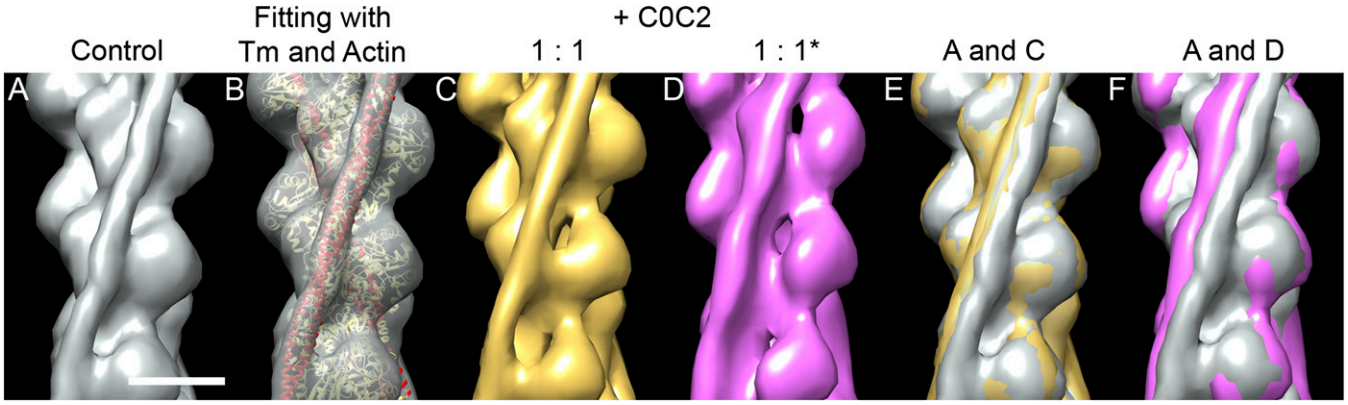

Fig. S4. 3D reconstructions of low Ca^{2+} reconstituted thin filaments decorated with C0C2 in different mixing orders. (*A*) Undecorated (control) filament. (*B*) Control filament fitted with ribbon depiction of F-actin. Tm atomic model in blocked state (actin monomers, yellow; Tm, red). (*C*) C0C2-decorated thin filament (A:C0C2 = 1:1), showing small shift of Tm as with native thin filaments (Fig. 4*B*). (*D*) When C0C2 was bound to actin before addition of Tm and Tn, Tm was shifted further, to approximately the closed position. (*E*, *F*) Superposition of *A* on *C*, and *A* on *D*, showing small movement (*E*) and large movement (*F*). (Scale bar = 5 nm.)

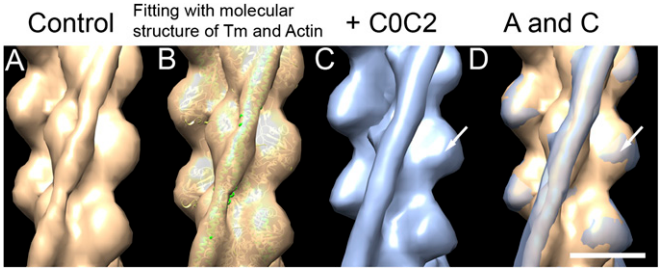

Fig. S5. 3D reconstructions of reconstituted thin filaments decorated with C0C2 under high Ca^{2+} conditions. (*A*) Undecorated (control) filament. (*B*) Control filament fitted with ribbon depiction of an F-actin. Tm atomic model in closed state (actin monomers, yellow; Tm, green). (*C*) C0C2-decorated thin filament (A:C0C2 = 1:3). (*D*) Superposition of *A* and *C*, showing little movement of Tm, which is located in both structures in the closed position. Extra density on SD1 of *C* (arrows in *C* and *D*) is presumably the proximal end of the bound C0C2. (Scale bar = 5 nm.)

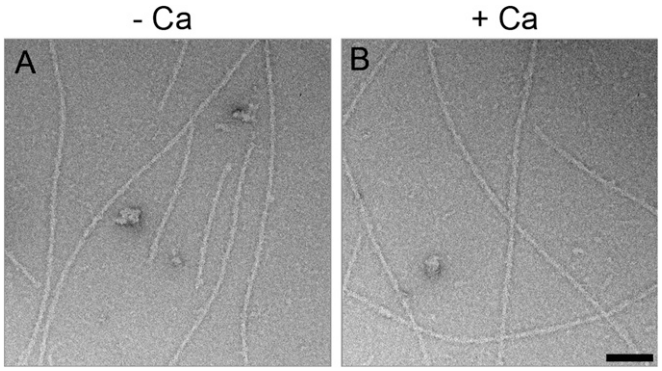

Fig. S6. Negative staining of C0C1f-decorated native thin filaments under low and high Ca^{2+} conditions at a 1:6 ratio of A:C0C2. (*A*) Low Ca^{2+} conditions. (*B*) High Ca^{2+} conditions. Both show wider filaments compared with control native thin filaments (Fig. 2*A*). (Scale bar = 100 nm.)

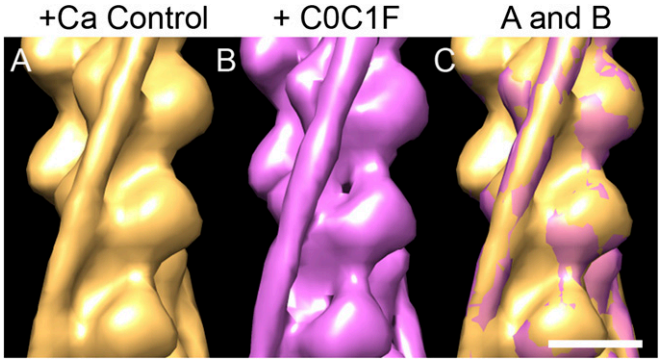

Fig. S7. 3D reconstructions of native thin filaments decorated with C0C1f under high Ca^{2+} conditions. (*A*) High Ca^{2+} control filament (yellow surface rendering). (*B*) C0C1f-decorated filament (pink). (*C*) Superposition of *A* and *B*, showing no Tm shift. (Scale bar = 5 nm.)

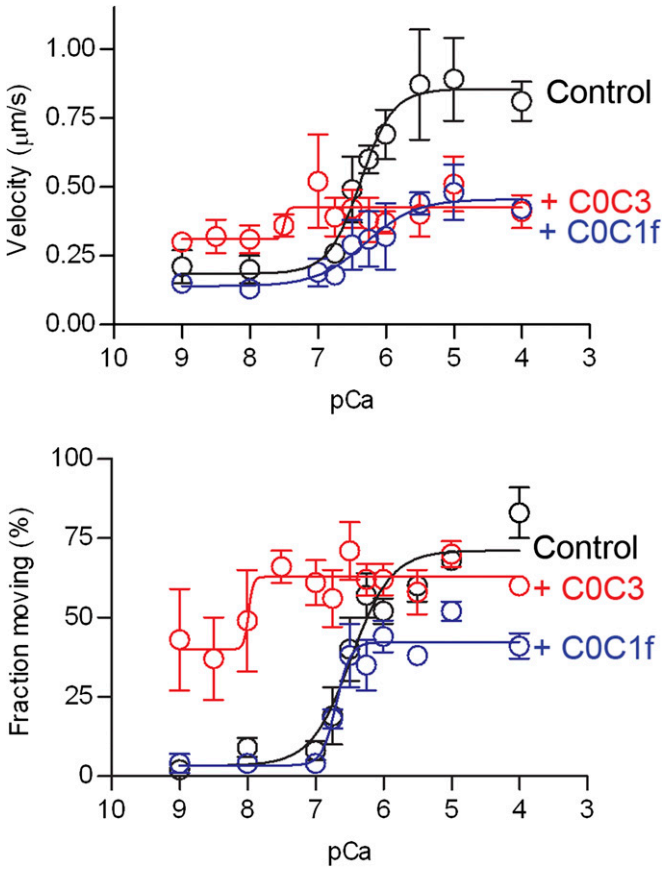

Fig. S8. Effect of N-terminal fragments on native thin filament pCa:velocity and pCa:fraction moving relations in in vitro motility assays. The black line shows native thin filaments demonstrating a sigmoidal response to Ca^{2+} in both velocity (*Upper*) and fraction of filaments moving (*Lower*). The red line shows that the presence of C0C3 increased the velocity and fraction of filaments moving at low Ca^{2+} but had a greater effect on the reduction of velocity than on the fraction of filaments moving at high Ca^{2+}. The blue line shows that the presence of C0C1f had no effect at low Ca^{2+} but reduced both the velocity and fraction of filaments moving at high Ca^{2+}. These results are summarized in Fig. 6, which shows effective activation (velocity × fraction moving vs. pCa).

Table S1. Diameters (nm) of thin filaments with or without C0C1f or C0C2 decoration (low Ca^{2+} conditions)

	Control	+ C0C2 (7: 1)	+ C0C2 (1: 1)		+ C0C2 (1: 3)	+ C0C2 (1: 6)	+ C0C1f (1: 6)
Reconstituted A.Tm.Tn	10.3 ± 0.7	11.6 ± 0.6	14.4 ± 1.3	14.3 ± 0.4*	17.1 ± 1.3	19.7 ± 1.3	15.5 ± 1.6
Native thin filament	10.5 ± 0.8	11.7 ± 1.0	14.5 ± 1.0		17.2 ± 0.7	20.1 ± 1.3	15.5 ± 1.5

Values are mean ± SD based on 20 of the filaments that had been selected for each reconstruction. For calculation of diameter, the SPIDER software package was used to obtain a density projection along the filament (after straightening). The diameter was calculated from the distance between the minima in the projection profile.

*In this experiment, C0C2 was mixed with F-actin, followed by Tm and Tn (in all other experiments, C0C2 was added to preformed thin filaments).